Transfer-gate region optimization and Pinned-Photodiode shaping for high-speed TOF applications

Fabio Acerbi[1], Manuel Moreno Garcia[1], Gözen Köklü[2], Bernhard Büttgen[2], Radoslaw Gancarz[2], Alice Biber[2], Daniel Furrer[2], David Stoppa[1]

[1] *Fondazione Bruno Kessler, Center for Material and Microsystems, Via Sommarive, 18, I-38123 Trento, Italy*
[2] *Heptagon Advanced Micro Optics Pte Ltd, Moosstrasse 2, CH-8803 Rüschlikon, Switzerland*
phone: +39 0461 314158, e-mail: acerbi@fbk.eu

***Abstract* – In this paper, we discuss potential optimizations of the structure and about the shape of pinned photodiodes (PPD) pixels for indirect-ToF sensors. We focus mainly on the transfer-gate (TG) region optimization (particularly pwell mask distance and the threshold adjustment implant) and on the PPD shape. TG region optimization is important to extract as fast as possible the charge from the PPD region. PPD shaping, instead, is important to quickly move the generated charge close to the TG, to be then collected by the floating diffusion. We also present experimental data on the produced 10µmx10µm-pitch pixels, introducing a setup for the direct measurement of the impulse-response-time, which takes into account both the TG transfer time and the photo-generated charge collection time. With the best pixel achieved during this study, we measured a quantum efficiency of about 45% at 850nm and a demodulation contrast of about 70% at 40MHz.**

I. Introduction

In recent years, there has been a massive development in 3D vision systems (i.e. range imagers), driven mainly by market requirements in gaming, automotive and mobile-systems applications. In such systems, Time-of-Flight (TOF) is emerging with respect to other techniques [1]. TOF relies on the measurement of time delay or phase shift between the light pulses emitted by the illuminator and the received backscattered light detected by time-resolved sensor (Fig 1 shows a representation of ToF working principle).

Several photo-detector technologies have been proposed in the literature for TOF applications including pinned photodiodes (PPD) realized in CMOS Image Sensor (CIS) processes [2][3]. PPDs feature several key advantages over other photo-detector technologies for TOF applications i.e. very compact pixel pitch enabling high-resolution imagers, lower dark current thanks to surface shielding and possibly less number of masks for CIS process customization compared to others. On the other hand, they are generally not easy to optimize for fast charge transfer, as required in TOF applications. There are typically two main targets for state-of-the-art iTOF pixels: i) de-modulation frequency in the order of 100MHz with good demodulation contrast and ii) more than 30% of Quantum Efficiency (QE) in the near infrared (NIR) wavelength region. In this work, we discuss the trends and required optimizations for development of such a PPD pixel and mainly focus on the optimizations for a fast photo-generated charge transfer from the photosensitive part toward the collection node.

II. Device Structure and Simulation Results

In this section, the device structure will be presented and

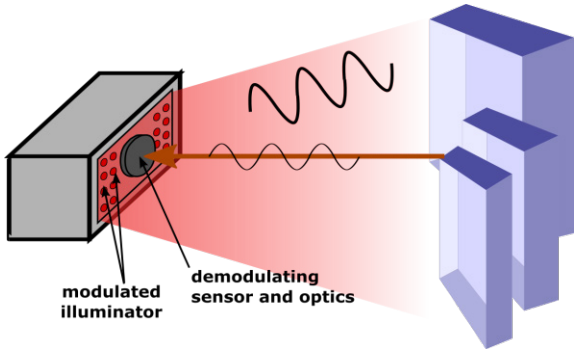

Fig 1 Basic principle of indirect Time-of-flight camera measurements: pulsed light is shined over the target and the camera demodulates the reflected light and created the 3D image.

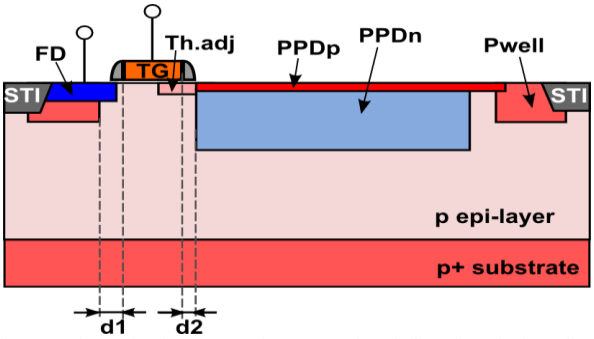

Fig 2 Schematized cross-section example of the pinned photodiode (PPD) structure, along the transfer-gate (TG) region. The different implants and the STI regions are highlighted: the n+ implant creating the floating diffusion (FD), the threshold adjustment implant, the p+ pinning layer (PPDp) and the storage n-well of the PPD (n-well customized for PPD) (PPDn). Distances "d1" and "d2" are critical for PPD performance.

three main optimization items are discussed for increasing the charge transfer speed together with TCAD simulation results: i) pwell to TG edge distance, which is d1 in Fig 2, ii) additional threshold adjustment implant, and iii) PPD shaping.

We employed a full 3D TCAD simulation deck, tailored and optimized for the specific manufacturing process that we used to produce the imaging chips. This is important to correctly simulate the effect of PPD shape and the current modulation between the two floating diffusions typically required in a PPD for iTOF sensor. However, to explain the optimization points in this chapter, we will focus on a simple 2D PPD structure, as shown in Fig 2. In this figure, the typical cross-section is represented, along with the most important implant regions.

First, we considered the optimization of pwell distance to TG edge. This is generally not deeply discussed in other

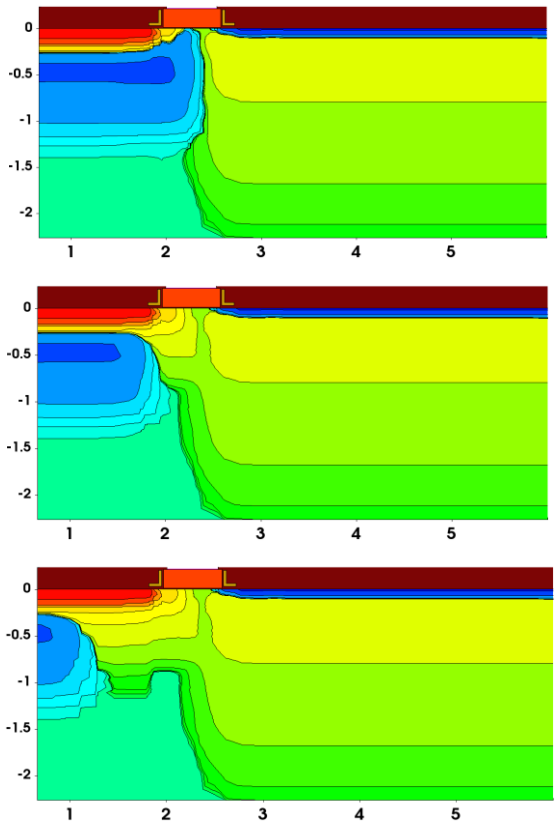

Fig 3 Doping concentration example, in the TG region, with different distance between p-well edge and TG edge. P-well mask self-aligned on TG (top), p-well mask to TG-edge distance of ~0.35µm (middle), and P-well mask farther from TG edge (bottom).

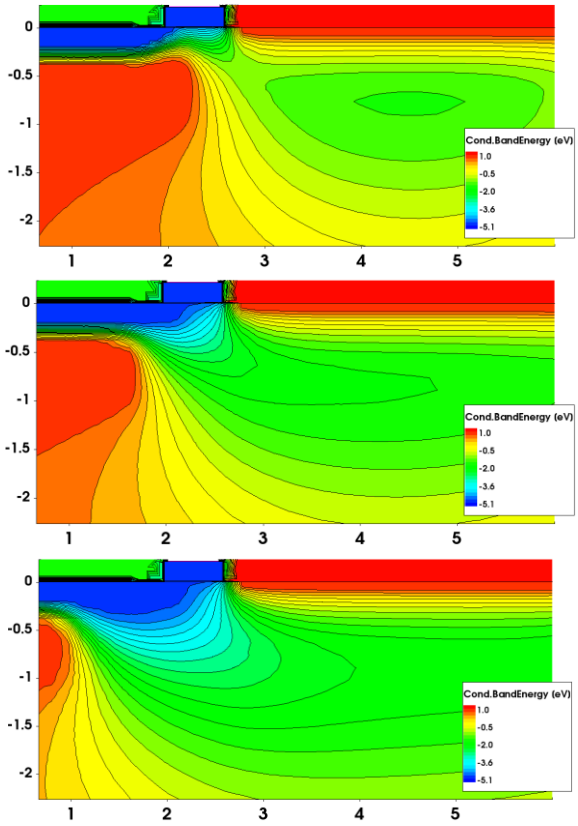

Fig 4 TCAD simulation of the conduction band energy, in the TG region, with different distance between p-well edge and TG edge, in the three cases of previous figure.

works, which instead may use other custom implants to avoid punch-through [4]. We report here the TCAD simulations with three different pwell distances: Fig 3 shows the doping concentration and Fig 4 represents the relative conduction band energy. Having p-well mask self-aligned on TG (first case) would results in a too small p-well to TG distance, creating a compression of the transistor channel and, in this case, preventing the correct biasing and full-depletion of the PPD itself. This will also slow down the transfer of the charge form the PPD. Conversely, a too high distance (third case) is preferable for the potential-lines distribution (from FD to PPD region), which will help in transfer speed reduction, but will decrease the effect of modulation in the TG channel, reducing the demodulation contrast. Thus, a good tradeoff needs to be found depending on the specific technology. In this case, this is represented by the second case.

Another point is the threshold adjustment implant: this can be particularly useful with high TG length, to create a higher potential barrier when TG is OFF, and to create a linear potential gradient from PPD to FD, when TG is ON [4][5], increasing the threshold in part of the TG region and speeding up the charge transfer. This can be done with a threshold adjustment implant all over the TG or by patterning its mask (see Fig 5). TCAD simulations results are reported in Fig 5, Fig 6, and Fig 7. Among all solutions, the approach with patterned threshold adjustment implant creates the most linear conduction-band energy variation, and avoids the presence of potential pocket as in the case without threshold adjustment implant.

III. PPD SHAPE

PPD shaping has also been analyzed, which is generally important for creating a fast charge drift towards the TG region. Generally, the drift field, still present at the edges of the PPD [6], is significantly reduced in the center. PPD shaping avoids this situation and also "pushes" the higher-potential region (inside the PPD) closer to the TG [7]: this is important to avoid potential barriers that would increase the transfer time. We investigated four different shapes: rectangular (as reference), triangular, convex and "bell"-shaped PPDs for analyzing the impact of PPD shape on charge transfer speed (see Fig 8). The PPD height to base ratio in all these structures is kept the same and approximately 1.5. Fig 8 shows the TCAD simulation of the conduction band energy inside the PPD. Convex shape has the advantage of maintaining a high FF and creating also a drift field towards the TG but the maximum of potential in the PPD is still too far from the FD. This creates a potential barrier in carrier path from PPD center towards the FD. Conversely, "bell"-shaped and triangular-shaped PPDs, creates a more linear pinning-voltage variation and the maximum of the potential is closer to the TG region. In the "bell"-shaped PPD it is the closest. This would result in a better potential gradient and a lower charge transfer time.

To compare the dynamic performance of these PPDs, we simulated the FD signal when introducing a pulsed illumination from the top of the PPD. We set a light pulse duration of hundreds of nanoseconds, and monitored how the FD current rises, when TG is ON. We obtained and

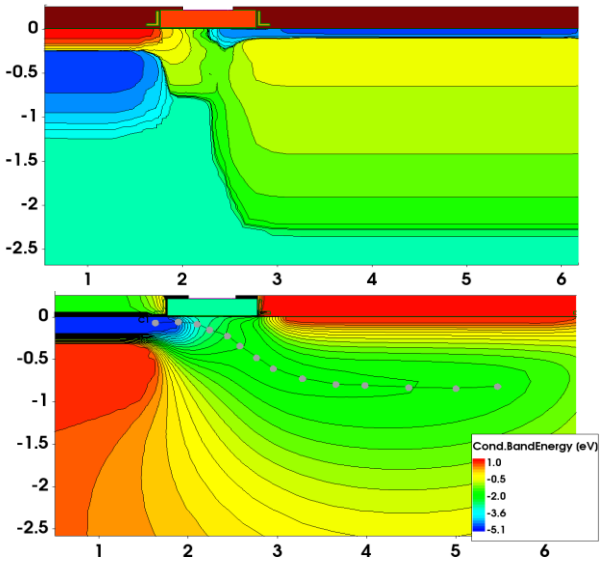

Fig 5 Doping concentration and conduction band energy, in the TG region, with the threshold adjustment implant. The Th. Adj. implant mask is covering the right part of the TG.

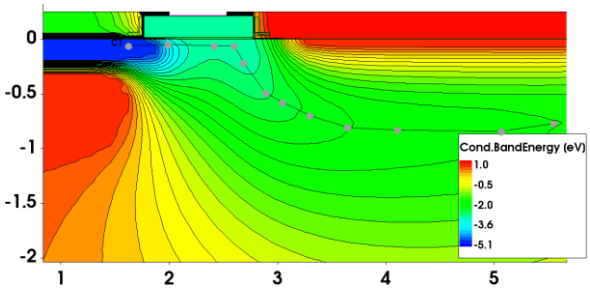

Fig 6 TCAD simulation of conduction band energy in the TG region, without any threshold adjustment implant.

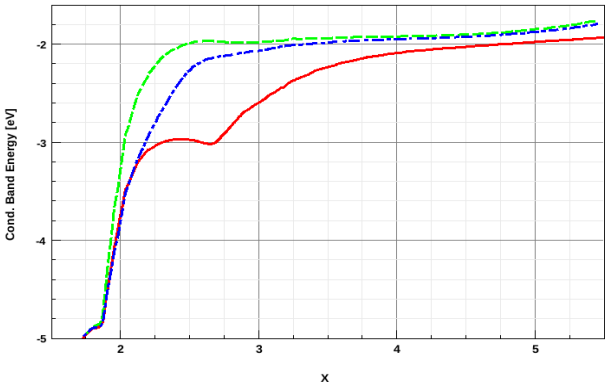

Fig 7 Conduction band energy along the cutline from FD to PPD center (as represented in Fig 5 and Fig 6), without (cont.) threshold adjustment implant, with this implant all over the TG (dash) and with implant only on PPD side (dash dot). The first case gives a small potential pocket, whereas the third case gives the most linear variation.

compared the photocurrent rise time 10%-90%, summarized in Table 1.

IV. MEASUREMENTS RESULTS

Based on TCAD simulations, we produced chips containing different version of PPDs arrays, with a pitch of 10µm x 10µm. We measured the quantum efficiency (QE) with a setup based on a broadband lamp, a monochromator and a calibrated photodiode. We obtained about 30% at 850nm and about 20% at 900nm.

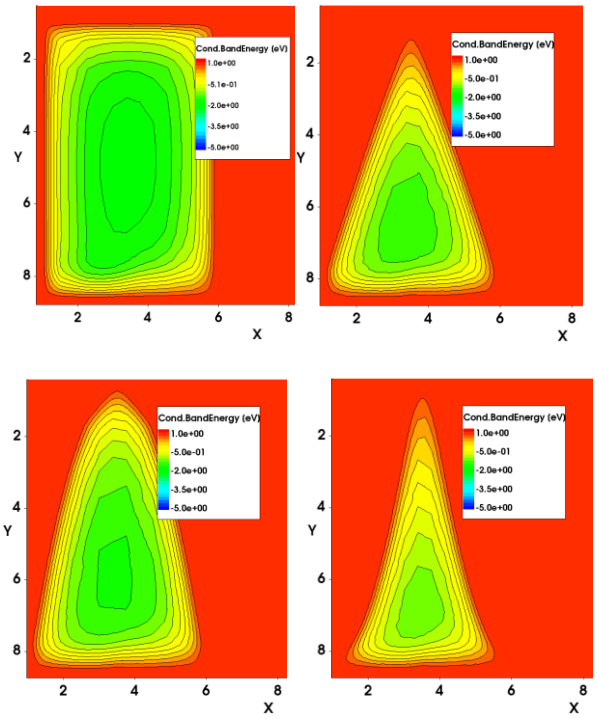

Fig 8 3D TCAD simulation: horizontal cutline (parallel to the surface) of conduction band energy (CBE) inside the shaped PPDs. In order: rectangular, triangular, convex and "bell" shape. It can be noted the different position od the minimum of CBE in the PPD region.

Another parameter is the demodulation contrast. When working in demodulation mode, it can be defined as [1][8]:

$$C_{demod} = \frac{meas\_Amp}{meas\_Offset} = \frac{\sqrt{(A_1 - A_3)^2 + (A_2 - A_4)^2}/2}{(A_1 + A_2 + A_3 + A_4)/4}$$

where A_n are the four different equally-spaced sampling points of the modulated photo-current. In this measurement, to isolate just the pixel demodulation contrast, we used a VCSEL modulated with an external fast-pulser, using a square-wave modulation pulse, synchronized with the acquisition system. We measured a contrast of ~64% at a frequency of 40MHz, for "bell"-shaped PPD.

As a particular measurement to validate the design methodology, we characterized also the impulse response time: this includes both the TG transfer time and the collection time for carriers from the epitaxial layer. The PPDs were operated in dynamic mode (toggling the two TGs on and off oppositely) with a frequency of 1MHz. We shined the detector with a sharp laser pulse (<100ps FWHM, λ=830nm) and we moved the laser excitation in time with respect to the TG toggling time (see the sketch in Fig 9). For each laser time-position, we collected the signal from the two FDs after the accumulation of several pulses. We plotted them as a function of the laser-pulse time delay, obtaining two curves that cross around the TG crossing time (see Fig 10). The speed of this transition (10%-90%) is the impulse response time of the PPD.

For the rectangular PPD in Fig 8, we measured a relatively high value, >300ns, mainly because of the high charge transfer time from the PPD to the FD. Conversely, for "bell"-shaped PPD we obtained 8ns impulse response

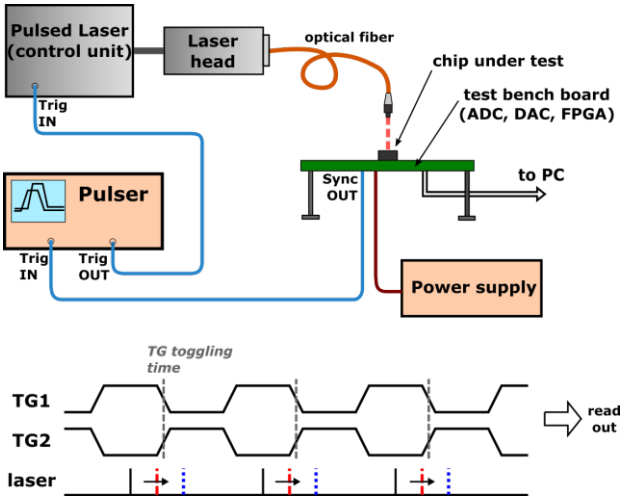

Fig 9 Setup for implulse response time measuremet. Sync signal from the test-bench-board (synchronous with TGs) is used to trigger the pulser, which, with an adjustable delay, triggers the laser pulse. The delay is changed, crossing the time when TG1 and TG2 toggle. Eventually, the FD signals as a function of time delay are plotted.

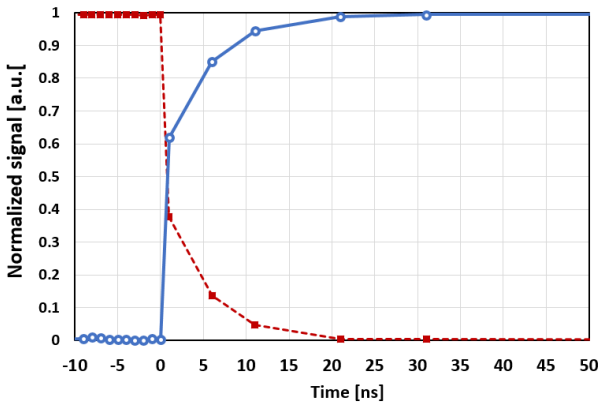

Fig 10 Measured impulse response of PPD bell-shaped, obtained with a laser excitation (<100ps FWHM, λ=830nm) and moving the laser excitation in time with respect to the TG toggling time. Normalized FD1 and FD2 signals are plotted. The rise time (10%-90%) is ~8ns.

Table 1 SUMMARY OF THE PERFROMANCE VARIATION (EXTRACTED FROM TCAD SIMULATIONS).

parameter	*Static contrast (%)*	*Impulse response time (10%-90%)*
p-well self-aligned	100%	> 500ns
Higher p-well distance	100%	0% (ref)
Much higher p-well dist.	50%	-11%
PPD shape: rectangular	100%	> 300ns
PPD shape: convex	100%	105ns
PPD shape: triangular	100%	9ns
PPD shape: bell	100%	8ns

time 10%-90%, as shown in Fig 10. This value is in agreement with the TCAD simulation results (see Table 1).

V. CONCLUSIONS

We discussed potential optimizations for PPD pixels designed specifically for ToF sensors. The TG region is very important to speed up the charge transfer. We focused on the pwell distance to TG, and on the threshold adjustment implant. The creation of drift field within the PPD region is also important: it can be achieved by shaping the PPD: here it is important to push the maximum potential region, in the PPD, towards the FD region. To optimize these points we make use of a custom 3D TCAD simulation deck. Main results are summarized in Table 1.

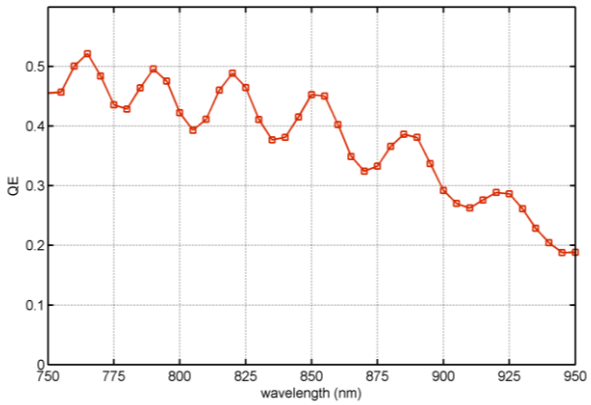

Fig 11 Measured QE of the PPD arrays, with 10µm x 10µm. Setup based on a broadband-lamp, a monochromator and a calibrated photodiode.

We produced and measured chips containing different arrays of PPDs, with a pitch of 10µm x 10µm. One promising PPD shape is the "bell"-shape PPD: with this shape, we measured 8ns impulse-response time, which includes both the TG transfer time and photo-generated carrier collection time.

All the optimizations described in this paper have been combined together leading to a final pixel with better performances. The QE has been further improved thanks to optimized silicon material: it is ~45% at 850nm and ~30% at 900nm (see Fig 11). The demodulation contrast, measured with the real-system illuminator is around 70% at 40 MHz and about 50% at 80MHz. This is thanks to the very low impulse-response time of about 3ns. We used a square-wave modulation, which is more and more approximates a sinusoidal function at high frequencies [8].

REFERENCES

[1] F. Remondino, D. Stoppa, "TOF Range-Imaging Cameras", Springer-Verlag Berlin Heidelberg 2013, 2013

[2] C. Tubert, et. al., "High Speed Dual Port Pinned-photodiode for Time-Of-Flight Imaging", Proc. IISW 2009, (Bergen, Norway).

[3] L.-E. Bonjour, et. al., "High-speed general purpose demodulation pixels based on buried photodiodes", Proc. of IISW 2011 (Hokkaido, Japan).

[4] Li Yiqiang et. al., "Charge transfer efficiency improvement of a 4-T pixel by the optimization of electrical potential distribution under the transfer gate", Journal of Semiconductors, vol. 33, no.12, Dec. 2012.

[5] E. R. Fossum et. Al., "A Review of the Pinned Photodiode for CCD and CMOS Image Sensors", IEEE J. electronic devices society, vol. 2, no. 3, May. 2014.

[6] Y. Xu, A. J. P. Theuwissen, "Image Lag Analysis and Photodiode Shape Optimization of 4T CMOS Pixels" Proc. of IISW 2013 (Snowbird, Utah USA).

[7] B. Shin, S. Park, H. Shin, "The effect of photodiode shape on charge transfer in CMOS image sensors", Solid state Electronics, 54, pp. 1416-1420 (2010).

[8] R. Lange et. al. "Demodulation Pixels in CCD and CMOS Technologies for Time-of-Flight Ranging", Proc. of SPIE Sensors, Cameras, and Systems for Scientific/ Industrial Applications II, vol. 3965, San Jose, (2000).